Nataraja Sekhar Yadavalli | Sarah Loebner | Thomas Papke | Elena Sava
Nicolae Hurduc | Svetlana Santer

A comparative study of photoinduced deformation in azobenzene containing polymer films

Suggested citation referring to the original publication:
Soft Matter (2016) 12, pp. 2593-2603
DOI http://dx.doi.org/10.1039/C6SM00029K
ISSN (online) 1744-6848

Soft Matter

PAPER

View Article Online
View Journal | View Issue

Cite this: *Soft Matter*, 2016, 12, 2593

A comparative study of photoinduced deformation in azobenzene containing polymer films†

Nataraja Sekhar Yadavalli,‡[a] Sarah Loebner,[a] Thomas Papke,[a] Elena Sava,[b] Nicolae Hurduc*[b] and Svetlana Santer*[a]

In this paper two groups supporting different views on the mechanism of light induced polymer deformation argue about the respective underlying theoretical conceptions, in order to bring this interesting debate to the attention of the scientific community. The group of Prof. Nicolae Hurduc supports the model claiming that the cyclic isomerization of azobenzenes may cause an athermal transition of the glassy azobenzene containing polymer into a fluid state, the so-called photo-fluidization concept. This concept is quite convenient for an intuitive understanding of the deformation process as an anisotropic flow of the polymer material. The group of Prof. Svetlana Santer supports the re-orientational model where the mass-transport of the polymer material accomplished during polymer deformation is stated to be generated by the light-induced re-orientation of the azobenzene side chains and as a consequence of the polymer backbone that in turn results in local mechanical stress, which is enough to irreversibly deform an azobenzene containing material even in the glassy state. For the debate we chose three polymers differing in the glass transition temperature, 32 °C, 87 °C and 95 °C, representing extreme cases of flexible and rigid materials. Polymer film deformation occurring during irradiation with different interference patterns is recorded using a homemade set-up combining an optical part for the generation of interference patterns and an atomic force microscope for acquiring the kinetics of film deformation. We also demonstrated the unique behaviour of azobenzene containing polymeric films to switch the topography *in situ* and reversibly by changing the irradiation conditions. We discuss the results of reversible deformation of three polymers induced by irradiation with intensity (IIP) and polarization (PIP) interference patterns, and the light of homogeneous intensity in terms of two approaches: the re-orientational and the photo-fluidization concepts. Both agree in that the formation of opto-mechanically induced stresses is a necessary prerequisite for the process of deformation. Using this argument, the deformation process can be characterized either as a flow or mass transport.

Received 6th January 2016,
Accepted 25th January 2016

DOI: 10.1039/c6sm00029k

www.rsc.org/softmatter

1. Introduction

Deformation of azobenzene containing polymer films under illumination with visible and ultraviolet light of locally varying intensity or polarization has been known since 20 years.[1,2] During this process polymer films can change their topography resulting in the formation of a surface relief grating (SRG);[3–9] when free standing, the polymer pieces can reversibly bend or contract under illumination and thus perform a mechanical work.[10,11] Irradiation with near field intensity patterns enables structuring of the photosensitive polymer films with a pattern of size far below the diffraction limit.[12–16] Since plenty of experimental and theoretical work are devoted to this process, one gets an impression that the SRG formation process is well understood. However, it is not the case. The main puzzling point here is how to explain a polymer mass transport over hundreds of nanometers within the glassy polymer film (far below T_g) without significant photo-induced softening of the polymer material. It was experimentally shown that under illumination there is a decrease in the Young's modulus and material viscosity, but only at maximum by a factor of four (from 3.4 GPa to 0.9 GPa under UV illumination).[17] This is the largest degree of softening known from the literature, while typical photo-induced softening was found to be in the range of several tens of percents.[18–21] However, when speaking

[a] *Department of Experimental Physics, Institute of Physics and Astronomy, University of Potsdam, 14476 Potsdam, Germany. E-mail: santer@uni-potsdam.de*
[b] *Department of Natural and Synthetic Polymers, Gheorghe Asachi Technical University of Iasi, Prof. Dimitrie Mangeron Street, 73, 700050-Iasi, Romania. E-mail: nhurduc@ch.tuiasi.ro*

† Electronic supplementary information (ESI) available. See DOI: 10.1039/c6sm00029k

‡ Present address: Nanostructured Materials Laboratory, The University of Georgia, 30602 Athens, Georgia, USA.

about thermal fluidization of the polymer material, one knows that the decrease in the mechanical modulus should be *ca.* 10^4 times when a polymer material undergoes a transition from a solid state to a fluid (melt) state.[22,23] Therefore, it is difficult to admit that the azobenzene containing material undergoes fluidization under illumination.[24,25]

On the other hand, some studies report that the azobenzene containing material undergoes photo-fluidization where the flow of the material is the main process of deformation.[18,25] The concept of photo-fluidization takes into consideration the continuous *trans–cis–trans* photo-isomerization cycles of the azobenzene groups (connected usually as side-chains to the polymer backbone) under the UV/Vis irradiation process. This continuous movement/switching of the azo groups induces conformational changes of the main chains, similar to the thermal movement of the macromolecules. However, it is difficult to estimate if the photo-induced chain movement has a similar effect inside the material as the thermal one.

What is clear is that the photo-isomerization of azobenzene molecules from a stable *trans*-state to a meta-stable *cis*-state during UV irradiation is an indispensable prerequisite for the polymer film deformation. Under multiple photo-isomerization cycles of the azobenzene groups, the molecules undergo re-orientation preferentially aligning with their main axis perpendicular to the electrical field vector. When incoming light has a local electric field vector distribution/modulation in terms of either intensity or polarization, achieved by using, for instance, two beam interference lithography, the formation of local phases of aligned azobenzenes and their coupling to the polymer matrix result in anisotropic photo-mechanical stress large enough to induce macroscopic deformation of the polymer material.[26–28] Recently it was reported that the stress within the polymer material could be as high as several hundreds of MPa.[29,30] Large opto-mechanical stress generated within polymer films is manifested by local scission of covalent bonds when polymer chains are covalently attached to a solid surface. In such polymer films the azobenzene molecules are attached either covalently or ionically to tethered polymer backbones forming photosensitive polymer brushes.[31–33] Under illumination with the interference pattern, at the areas where the polymer materials is escaped from, the polymer chains are ruptured from the solid surface.[34] Even when the metal layer or multilayered graphene is deposited on top of a photosensitive polymer film, opto-mechanical stress generated during illumination is enough to not only deform the polymer material but also to rupture the metal layer and stretch the graphene multilayer.[26,29] Acquiring a shift of the G-band adsorption peak of the stretched graphene along the topography grating using Raman microcopy, we have shown that the value of local opto-mechanical stresses can be as high as 1 GPa.[29] It is obvious that the fluidized polymer material would not be able to rupture metal layers and deform the covalent bonds of graphene.

We think that a recently proposed theoretical approach based on the development of anisotropic opto-mechanical stresses within the polymer material during azobenzene and polymer backbone reorientation is a more viable working hypothesis to explain light induced polymer film deformation.[35–38] This approach involves analytical calculations[38] as well as computer simulations[37] where molecular details of the azobenzene–polymer structure described in terms of the angle between the azobenzene main axis and the polymer backbone are considered to explain the deformation of the polymer material and to calculate mechanical stresses needed for this deformation. The opto-mechanical stress calculated within this approach is *ca.* 130 MPa, which is larger than the typical yield stress of the glassy polymer ($\sim$50 MPa for PMMA). This stress can thus induce significant deformation of the glassy photo-sensitive polymer film without the need for the photo-fluidization process.

One of the main achievements of the orientation concept is the ability to explain how the direction of the mass transport towards or away from the light intensity depends on the molecular details of azobenzene coupling to a polymer backbone. Using the angle between the azobenzene containing side chain and the backbone one can predict whether the polymer material elongates or contracts along the electrical field, *i.e.* goes into intensity maxima or minima.[39]

The orientation concept is especially useful to explain polymer film deformation under irradiation with interference patterns of constant intensity but locally varying polarization, the so-called polarization interference pattern (PIP). At constant intensity of incoming light, it is difficult to understand anisotropic deformation of the polymer film, even under the assumption of polymer photo-fluidization. Experimentally, it is also not trivial to assign the electrical field vector distribution of the polarization interference pattern to the topography variation. For this purpose we have recently proposed a set-up consisting of an optical part for the generation of different interference patterns coupled to an AFM for the simultaneous acquisition of a polymer topography response on changing the local electric field distribution of interference patterns.[40–43] With this set-up it is possible to record the kinetics of SRG growth for different interference patterns, and to study how the change in the local distribution of the electrical field vector under switching between different polarization of interfering beams influences the topography variation in the polymer film.

Here we report on light induced structuring and deformation of three polymers differing in their glass transition temperatures. Two of them have the same azobenzene compound attached as a side chain to two different backbones: the flexible polysiloxane (Azo-Psi) and the rigid poly(chloromethylstyrene) (Azo-PCMS) main chain. The glass transition temperatures are 32 °C and 87 °C for Azo-Psi and Azo-PCMS, respectively. The third polymer (PAZO) has a different azobenzene side chain but comparable with Azo-PCMS glass transition temperature (T_g = 95 °C). To inscribe SRG, the polymer films were irradiated with interference patterns of different polarizations: intensity interference patterns (IIPs: SS, PP, RR, LL) and polarization interference patterns (PIPs: $\pm$45°, RL). The irradiation was conducted *in situ* while simultaneously acquiring the topography change using AFM. The polymers of different glass transition temperatures show comparable kinetics of topography change and maximally attainable grating height under irradiation with intensity interference patterns (IIPs). The illumination with polarization interference patterns (PIPs) results in a higher grating height for all three polymers,

but a more pronounced topography change was found for the polymers of higher glass transition temperature. Thus the maximal grating height for the polymers Azo-PCMS and PAZO structured with PIP is *ca.* 3 times higher than in the case of Azo-Psi.

We have also performed experiments where a rectangular piece of a polymer film was isolated out of the film using AFM lithography and irradiated with homogeneous light of linear polarization. For all three polymers we have found that the rectangular piece elongates along the electrical field vector and contracts in the perpendicular direction.

2. Materials and methods

2.1 Photosensitive materials

Azo-Psi (Fig. 1). Fig. 1 Synthesis of the polysiloxane containing chlorobenzyl groups in the side-chain takes place in a two-step reaction, starting from dichloro(4-chloromethylphenylethyl)-methylsilane. In the first step a hydrolysis reaction occurs, with the formation of a mixture of linear and cyclic oligomers. The second step supposes a cationic equilibration of the cyclic and linear oligomer mixture in the presence of triflic acid and 1,3-divinyl-1,1,3,3-tetramethyldisiloxane as chain blockers, resulting in the formation of linear polymers ($M_n \sim 6000$ g mol^{-1}). The polysiloxane containing chlorobenzyl groups is then modified with 4-phenylazophenol by a SN2 reaction (DMSO solvent). The details of polysiloxane synthesis and characterization can be found elsewhere.[44]

Azo-PCMS (Fig. 1). Poly(chloromethylstyrene) was obtained using radical polymerization in solution (benzene) at 80 °C, using 2,2′-azoisobutyronitrile as an initiator ($M_n \sim 5000$ g mol^{-1}). Poly(chloromethylstyrene) was modified in a second step with 4-phenylazophenol under similar reaction conditions as in the case of polysiloxanes.

PAZO. An azobenzene-containing photosensitive polymer (poly(1-[4-(3-carboxy-4-hydroxyphenylazo)benzenesulfonamido]-1,2-ethanediyl sodium salt)), shortly named as PAZO, is purchased from Sigma-Aldrich. The chemical structure of PAZO is shown in the inset of Fig. 1. The polymer solution is prepared by dissolving PAZO in a mixture of 95% methoxy-ethanol and 5% ethylene glycol. The molecular weight of PAZO is estimated by GPC analysis to be $M_n = 1.4 \times 10^4$ g mol^{-1} (*ca.* 40 repeat units).

2.2 *In situ* AFM connected optical setup

To achieve the photoinduced deformation in polymer films, single beam and two beam interferometer irradiation is used. A continuous wave-diode pumped solid state laser (CW-DPSSL, 75 mW output power) operating in a single longitudinal mode with a wavelength of 491 nm and oscillating in the vertical linear polarization state (↕) is used (Cobalt Calypso™) for both setups. The laser beam is spatially expanded and then collimated with a pair of focusing and collimating lenses, and a pinhole system. For single beam irradiation, a half wave plate and a polarizer are placed after the pinhole system to control the polarization state of the beam. The uniform 5 mm diameter central part of the collimated Gaussian beam profile is aligned at the polymer sample positioned with the AFM (PicoScan, Agilent, USA) for *in situ* measurements as shown in Scheme 1a. For the two beam interferometer, a 50 : 50 (L : R) beam splitter is placed after the pinhole to separate the single beam into two beams with fairly equal intensities. The beams then pass through a set of wave plates and polarizers and are made to interfere near the sample as shown in Scheme 1b. The wave-plates labelled 'a' and 'b' are employed to control the intensity of beams passing through the polarizers (P_1 and P_2) based on Malus's law.

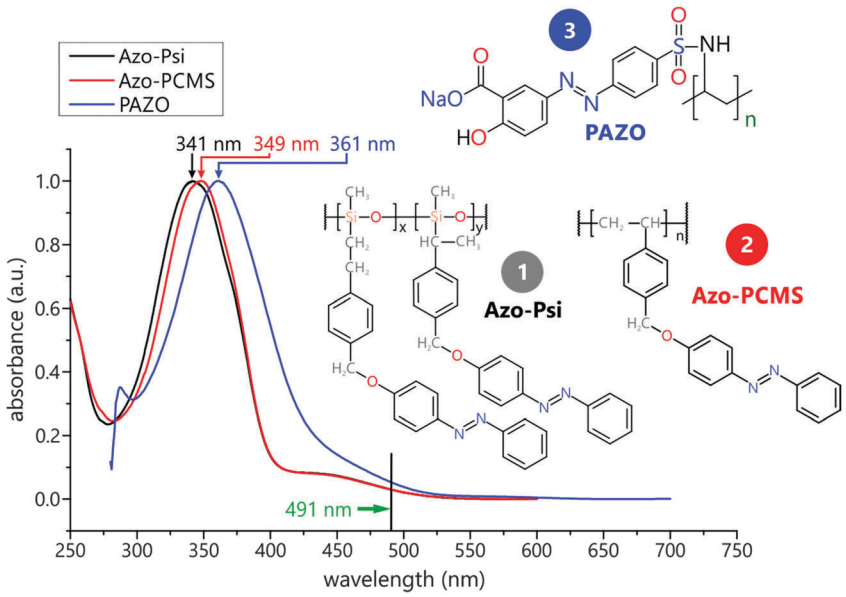

Fig. 1 UV-Vis absorption spectra and the chemical structure of (1) Azo-Psi (black), (2) Azo-PCMS (red) and (3) PAZO (blue). The irradiation wavelength of 491 nm is marked by a green arrow in the absorption spectra.

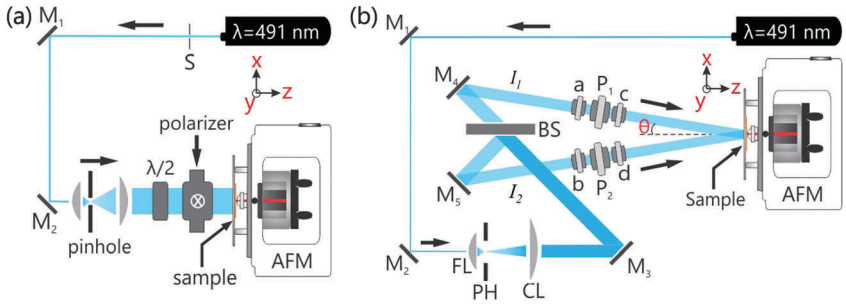

Scheme 1 Experimental setup. (a) Scheme of a homemade set-up connecting an AFM and an optical part. M_1 and M_2 are mirrors. A half wave plate ($\lambda/2$) and a polarizer are used to control the polarization state of the beam. Circled cross mark on the polarizer represents the direction of the transmission axis of the polarizer (vertical linear polarization, ↕). (b) *In situ* two-beam interferometric atomic force microscopy (IIAFM) used for inscribing the surface relief gratings (SRGs). FL – focusing lens; PH – pinhole; CL – collimating lens; (a and b)-half wave plates; (c and d)-either half wave or quarter wave plates and/or their combinations. P_1 and P_2 – polarizers; AFM – atomic force microscope; S – computer controlled beam shutter; M_1 to M_5 – mirrors; BS – 50/50 beam splitter; I_1 and I_2 – intensity of the beams.

Irradiation of polymer films is done from the glass side, while topography changes of the polymer are recorded using an atomic force microscope (AFM). All *in situ* AFM measurements were performed with 1 Hz scan speed, 512 scan lines per micrograph and each micrograph requires 9 min to complete. The AFM scan cycle is toggled to maintain continuous up- and down-scanning during *in situ* measurements so that each scan line running upward or downward in the AFM micrographs represents the topography variations in the whole polymer film as a function of irradiation time.

3. Results and discussion

3.1. Kinetics of polymer film deformation during irradiation with intensity (IIP) and polarization interference patterns (PIPs)

We compare here the reaction on irradiation of three different photosensitive polymers: (1) Azo-Psi, (2) Azo-PCMS and (3) PAZO (Fig. 1). First two polymers have the same azobenzene compound attached as a side chain to two different backbones: Azo-Psi has a flexible polysiloxane and Azo-PCMS is with a rigid poly(chloromethylstyrene) main chain. The difference in the nature of the backbone results in the large difference in the polymer glass transition temperature, T_g, to be 32 °C and 87 °C for Azo-Psi and Azo-PCMS, respectively, (Table 1). The third polymer PAZO has the highest T_g of 95 °C.[45] Fig. 1 shows the UV-Vis absorption spectra of the polymers. In the case of Azo-Psi and Azo-PCMS polymers the *trans*-state is characterized by the absorption band (π–π* transition) with maximum at 341 nm and 349 nm, respectively, while the *cis*-state has a characteristic adsorption peak situated at 442 nm (n–π* transition). The thermal relaxation of the *cis*-isomer takes place within *ca.* 30 hours.

Table 1 Molecular parameters of the studied polymers

	Photosensitive polymer	Substitution degree (%)	M_n (10^3 g mol^{-1})	T_g (°C)
1	Azo-Psi	85	10.3	32
2	Azo-PCMS	98	11.8	87
3	PAZO	100	14.0	95

In the case of PAZO the absorption band of the *trans*-state is observed at 361 nm, while the n–π* transition is partially buried beneath the trans-adsorption band (Fig. 1, blue curve). The polymers were irradiated with the blue light of λ = 491 nm (I = 100 mW cm^{-2}) either with a homogeneous intensity distribution or with an interference pattern of different polarizations and intensities. At this wavelength both *trans*- and *cis*-states adsorb, so that under illumination azobenzene undergoes multiple transitions and both types of isomers coexist.

With our homemade set-up it is possible to record locally the kinetics of the SRG height growth for different polarization combinations. Fig. 2 shows how the SRG height changes with irradiation time for different polarization combinations of two interfering beams for polymers: Azo-Psi (Fig. 2a) and Azo-PCMS (Fig. 2b). PAZO is comprehensively investigated in this respect in our previous publications.[40,42] The maximal SRG height of all polymers is obtained in the case of the polarization interference pattern (PIP) (±45°, and RL), while irradiation with the intensity interference pattern (IIP) results in lower SRG height.

For the case of the polymer with low T_g (Azo-Psi), the topography change appears rapidly within the first 15 minutes of irradiation under both PIP and IIP illumination conditions followed by the saturation (Fig. 2a). The maximum SRG height at saturation depends on the polarization combination: the smallest grating height developed at SS (IIP) polarization combination is 3 nm followed by LL and RR of 55 nm and PP (IIP) combinations of 100 nm SRG height. Irradiation with PIP (RL and ±45°) combinations results in SRG maxima of 200 nm. Upon IIP illumination a similar trend in the reaction is observed for the polymer Azo-PCMS of higher T_g (Fig. 2b). Irradiation with polarization interference patterns results in a higher SRG height at saturation: 500 nm (RL) and 400 nm (±45°) (Fig. 2b). The saturation of the SRG growth starts after a longer irradiation time of 60 minutes. In the case of the PAZO polymer, the maximal grating height is also achieved during irradiation with polarization interference patterns (see Fig. S1, ESI†), however, the kinetics of grating growth differs from Azo-Psi and Azo-PCMS, the SRG height growth is observed to be gradual during the 10 hours of irradiation.[40] However, the reaction of PAZO on

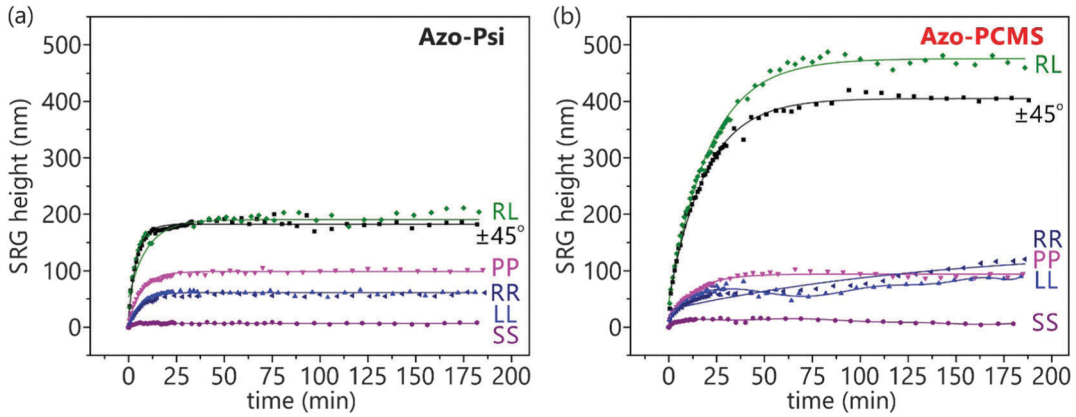

Fig. 2 SRG growth kinetics of (a) Azo-Psi and (b) Azo-PCMS films for different polarizations and intensity modulated interference patterns: PP, RR, LL and SS are intensity interference patterns (IIPs), RL and ±45° are polarization interference patterns (PIPs).

irradiation with an intensity interference pattern is similar: there is a rapid growth within first 30 minutes followed by saturation.[40]

When comparing the reaction of all three polymers to irradiation with an intensity interference pattern of PP polarization combination, which gives the largest SRG height for IIP, one clearly infers that the polymers show similar growth kinetics and saturation value of grating height (Fig. 3b). The comparison of the reaction on irradiation with the polarization interference pattern (PIP, shown for ±45°) (Fig. 3a) infers two different kinetics for SRG change. The polymers Azo-Psi and Azo-PCMS react rapidly on irradiation achieving saturation after 15 and 60 minutes of irradiation, respectively. The SRG height of the PAZO polymer increases gradually up to 220 nm during 600 minutes of irradiation (Fig. 3a, blue curve). The continuous SRG growth within the PAZO implies the existence of the extended mechanical stresses within the film. Since both polymers have similar T_g, molecular weights, and the degree of substitution with azobenzene groups, the different kinetics of PAZO and Azo-PCMS deformation during PIP irradiation is most probably due to different photochromic behaviour of the azobenzene groups. In the case of PAZO, the absorption bands (maximum absorption at 365 nm) of the *trans*- and *cis*-isomers overlap such that under irradiation there are successive photo-isomerization transitions between the two isomers, resulting in a rotational motion of the side chains. The PIP ±45° pattern exhibits alternating local areas of horizontal, circular and vertical polarizations. In the areas of circular polarization a continuous rotation of the side chains takes place, while in the adjacent regions packing of azobenzenes into local phases occurs over time, during which azobenzene molecules orient differently.

This process lasts longer for PAZO than for the other two polymers, since thermal relaxation of the *cis*-isomer of Azo-Psi and Azo-PCMS polymers takes place within *ca.* 30 hours. Indeed, under illumination there is a competition of three photo-isomerization effects: (i) transition from the *trans*- to *cis*-state, (ii) thermal relaxation to the trans state, and (iii) cis conversion upon light absorption. Although under illumination with 491 nm both *trans*- and *cis*-isomers of all three polymers adsorb, the thermal relaxation of the *cis*-isomer in the case of Azo-Psi and Azo-PCMS takes several hours, while PAZO *cis–trans* transition occurs within a time interval shorter than a second. This means that if all other conditions remain the same, the Azo-Psi and Azo-PCMS polymers should achieve a photostationary state,

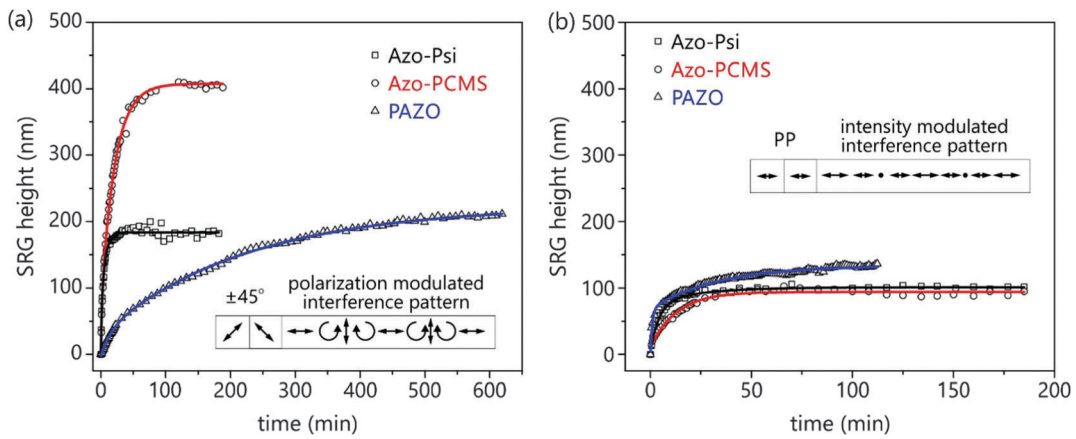

Fig. 3 Comparison of SRG growth kinetics in Azo-Psi (black), Azo-PCMS (red) and PAZO (blue). (a) Growth kinetics for a ±45° interference pattern (PIP). (b) Growth kinetics for a PP interference pattern (IIP).

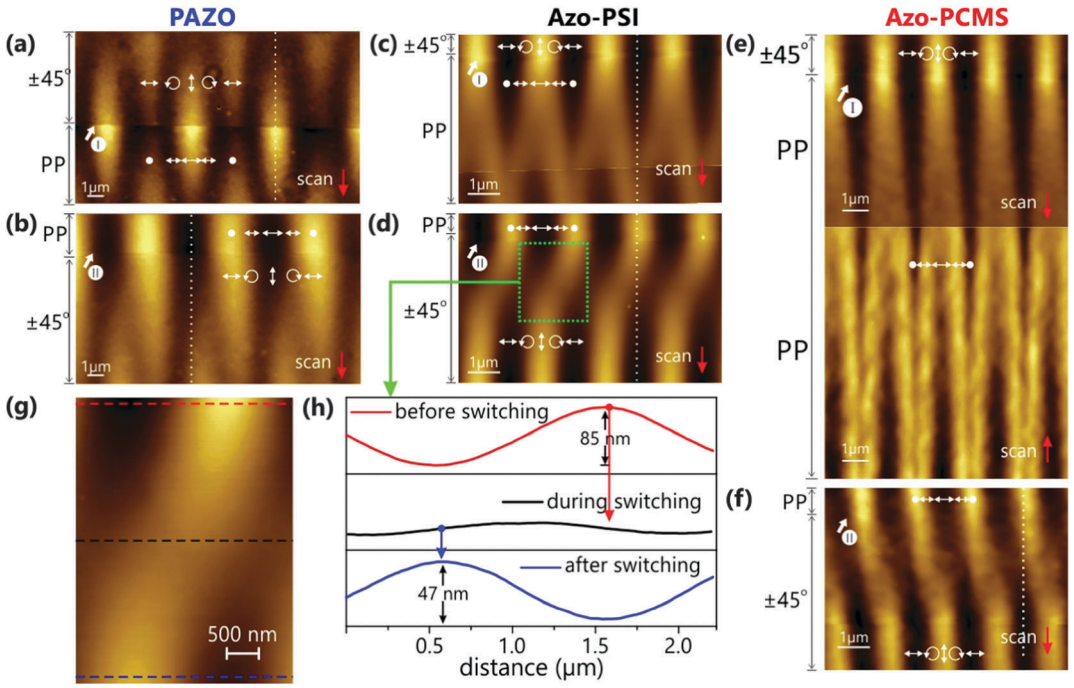

Fig. 4 Switching experiments: a comparison of SRG formation in PAZO (a and b), Azo-PSI (c and d) and Azo-PCMS (e and f) films under irradiation with ±45° and PP interference patterns. (a, c and e) During scanning from top to bottom at the place marked by thick white arrow "I" the irradiation conditions were changed from ±45° to PP interference patterns. (b, d and f) At the position marked by thick white arrow "II" the interference pattern was changed back to ±45° polarization combination. The distribution of the electrical field vector relative to the topography variation is shown by white arrows. (g) Enlarged area from (d) shows the details of the topography switching. (h) The cross-sections of the polymer topography acquired before switching (red line acquired along the red dashed line in g), after switching (blue line) and at the point of flattened topography (black line acquired along the black dashed line in g).

with a steady-state *trans–cis* composition faster than within the PAZO polymer. This difference might be one of the reasons for the fast saturation kinetics of SRG growth within Azo-Psi and Azo-PCMS. Taking into account that the opto-mechanical stresses are generated during local re-orientation of the azobenzenes and subsequent alignment of the polymer backbones, one infers that the gradual growth of the SRG in the PAZO film is related to a continuous development of the stress under multiple *trans–cis–trans* switching.

We should mention that the maximally achievable SRG height within a certain polymer at fixed polarization combinations strongly depends on the thickness of the polymer film and the periodicity of the interference pattern. In Fig. S1, ESI,† we present as an example, the dependence of SRG height on grating periodicity and film thickness for the PAZO film irradiated with ±45° interference patterns. Therefore, in order to be able to perform a comparison between the behavior of different polymers, in this paper we fixed the thickness of the polymer film and the periodicity of the interference pattern at 500 nm and 2 μm, respectively.

Summarizing this part, we can say that it is evident from the above discussed results that the kinetics and the extent of topography change induced during irradiation with intensity interference patterns (IIPs) do not significantly differ for three polymers studied here. However, the extent of topography change as a reaction to irradiation with polarization interference patterns (PIPs)

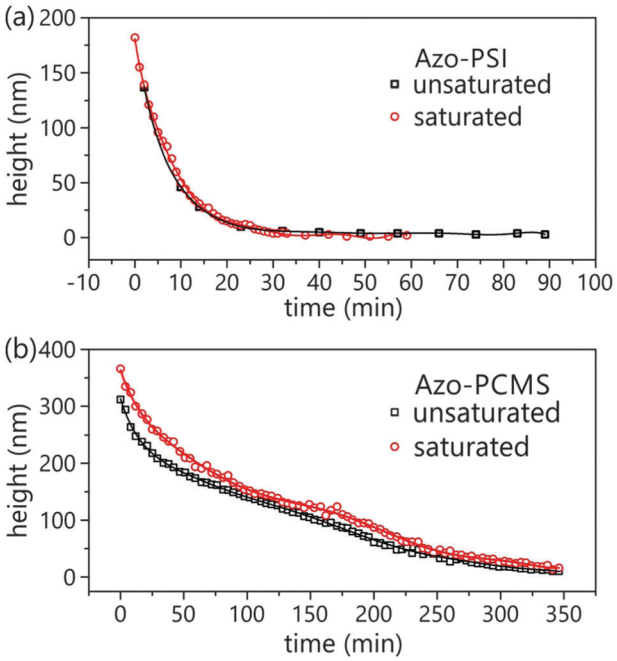

Fig. 5 SRG height as a function of irradiation time for two polymers: (a) Azo-PSI and (b) Azo-PCMS. First the SRG was inscribed using ±45° polarization patterns either to the saturation height (red curves) or to the height value before the saturation (black curves), afterwards the irradiation was switched to the SS polarization, and the decrease in the height is recorded over irradiation time.

is more pronounced for the polymer with higher T_g, *i.e.* Azo-PCMS. Presumably, Azo-Psi of lower T_g exhibits weaker elastic coupling between the polymer main chain and active azobenzene side chains reorienting under irradiation. Indeed, since the reorientation mechanism of both azobenzene side chains and backbones is responsible for the overall film deformation, the mechanism of energy transduction from the active azobenzene groups to the passive polymer backbone should determine the efficiency of the SRG growth while keeping the remaining parameters similar. For instance, depending on how the azobenzenes are attached to the host polymer matrix, *e.g.*, simple non-bonded mixtures, ionic or covalent attachment, one expects varying SRG efficiency.[38] In our case, the azobenzenes are attached covalently to the backbone, but the length of the spacer between the azobenzene side chains of Azo-Psi (lower T_g) is longer than the length of the spacer of the other two polymers. We believe that this can be the reason (together with the flexible backbone of the Azo-Psi) for the weaker response to irradiation. For an exact picture of the link between the sub-atomic level (quantum-mechanical photoisomerisation) and macroscopic light-induced deformation of the sample one has to conduct computational studies of azobenzene polymers with atomistic detail, which is however out of the scope of the present work.

3.2. Reversible switching of the polymer film topography during changing of irradiation conditions

Using our combined set-up we are able to follow the reaction of the polymer topography on changing the nature of the interference pattern *in situ* (Fig. 4).[42] For all three polymers irradiation was initiated with $\pm 45^\circ$ interference patterns (PIPs). As it can be seen in Fig. 4, the topography maximum develops at the position where the local electrical field vector has a vertical orientation in all three cases (see white arrows in Fig. 4). The variation of the electrical field vector distribution along the topography for different polarization combinations is shown in Fig. S2, ESI.† The protocol for ascribing the electrical field vector distribution to the topography variations is described elsewhere.[25–28,46,47]

Upon exposure of the polymer films to irradiation with $\pm 45^\circ$ interference patterns and the simultaneous acquisition of the topography development, the polarization was switched to the PP interference pattern, the position of irradiation change is marked by thick white arrows in Fig. 4. In the following 4 minutes the positions of the topography maxima and minima were interchanged: the topography maximum develops where the intensity was minimum (see Fig. 4). In the case of PAZO, the interchange is direct, *i.e.* the previously developed maxima flattened with

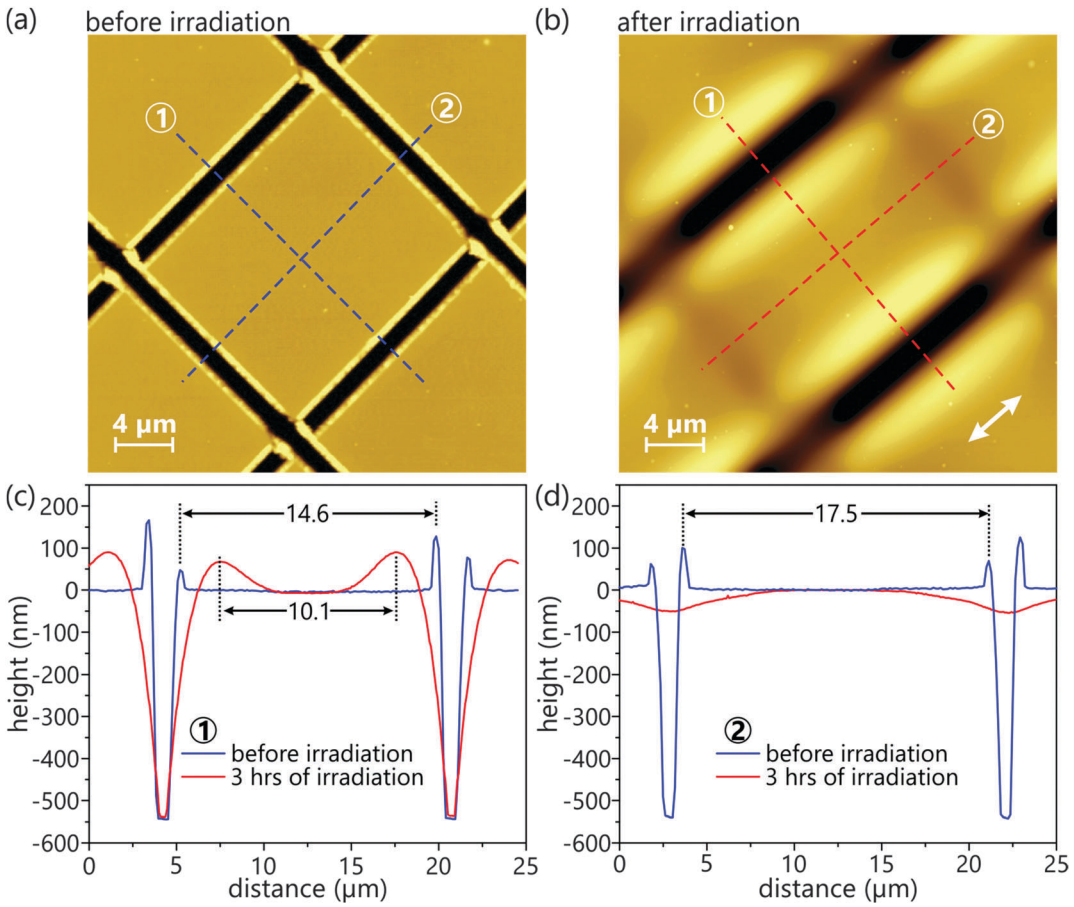

Fig. 6 Polarization dependent mass-transport of Azo-PSI. (a) A rectangular piece cut out of a polymer film using AFM tip lithography is shown before irradiation. (b) Topography of the Azo-PSI film after irradiation. (c) and (d) AFM cross-sectional analysis of the rectangular width before (blue curve) and after (red curve) irradiation. The direction of the polarization is marked by the white arrow.

irradiation time, while the maxima grow gradually where the previous topography minima developed (Fig. 4a). The topography maxima of two other polymers, Azo-Psi and Azo-PCMS, appear to be split into two halves which then merge into new maxima (Fig. 4c and e). This kind of impression is an optical illusion. Indeed, since the AFM micrograph does not provide with the simultaneous snapshot of the topography change over the whole scanned area, but is acquired line per line, at certain kinetics of the flattening of one peak and the growth of another, one gets images like shown in Fig. 4c and e. Cutting a thin slit out of Fig. 4d (green colour box) one finds that at certain irradiation time the film topography continued flattening while the development of the new maxima and minima sets in (Fig. 4g and h).

The same behaviour is observed when switching from the ±45° interference pattern to SS polarization combination (Fig. 5). In these experiments we have inscribed SRG up to a saturation height using ±45° polarization combination: 200 nm for PAZO, 180 nm for Azo-Psi and 350 nm for Azo-PCMS, followed by irradiation with an SS interference pattern. In all three cases the topography maximum shifted by half a period and develops up to the saturation height for the SS polarization. For the case of the polymers Azo-Psi and Azo-PCMS, the grating height is quite small to be 3 nm and 10 nm, respectively, (see Fig. 2). Thus, summarizing this part we can state that reversible switching of the topographies shown in Fig. 4 and 5 indicates visco-elastic behaviour of the polymer film.

3.3. Deformation of the piece of the polymer film under irradiation with linearly polarized light of homogeneous intensity

One of the main experiments that is thought to support the concept of photo-fluidization is the erasure of a scratch within the polymer under irradiation with light of polarization pointing perpendicularly to the scratch.[17] To check whether this is the case for our polymers, we have performed similar experiments, but the polymer film was scratched in such a way that it forms a rectangular piece cut/isolated out of the whole film (Fig. 6). Fig. 6 shows polymer 1 (Azo-Psi) with the lowest T_g (Table 1). Irradiation was performed with the light of 491 nm (I = 100 mW cm^{-2}) and polarization pointing along the longer axis of the rectangle (the polarization direction is marked by the white arrow in Fig. 6). After 3 h of irradiation, as expected, one of the grooves is closed, but the second groove appears to have a larger width than before irradiation (Fig. 6b). By measuring the size of the rectangle, we have found that the length increased from 16.9 μm to 18.7 μm, and the width decreased from 14.7 μm to 10.1 μm (Fig. 6c). As reference points for measurement of the width, we choose the distance between topography maxima as shown in Fig. 6c.

Because of the adhesion forces between the bottom side of the film and the solid surface, the bottom layer of the film do not move during irradiation, but the upper layer compresses towards the rectangular centre. The cross-sectional area before and

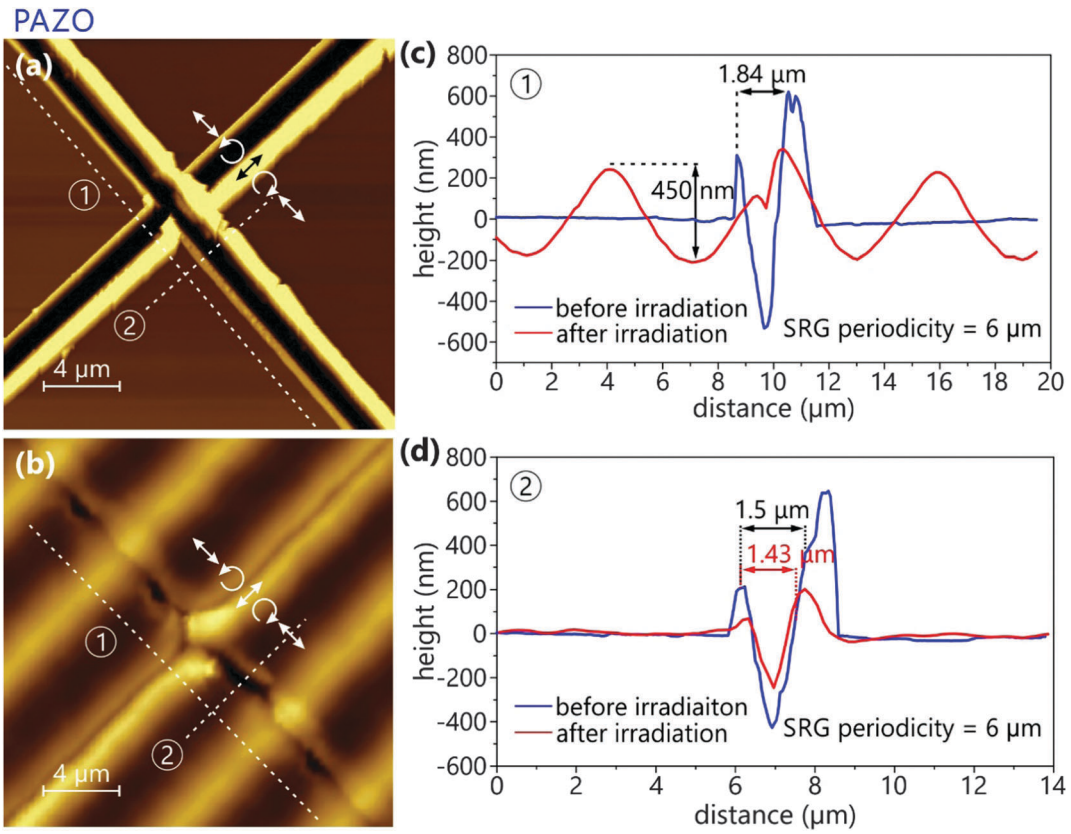

Fig. 7 (a) AFM micrograph of the crossed grooves scratched in the PAZO film before irradiation. (b) PAZO film topography in the scratch regions after irradiation with interference patterns (±45°). The distribution of the E-field vector relative to the SRG is shown by the black arrows. (c) A comparison of cross-sections labelled 1 in (a) and (b). (d) A comparison of cross-sections labelled 2 in (a) and (b).

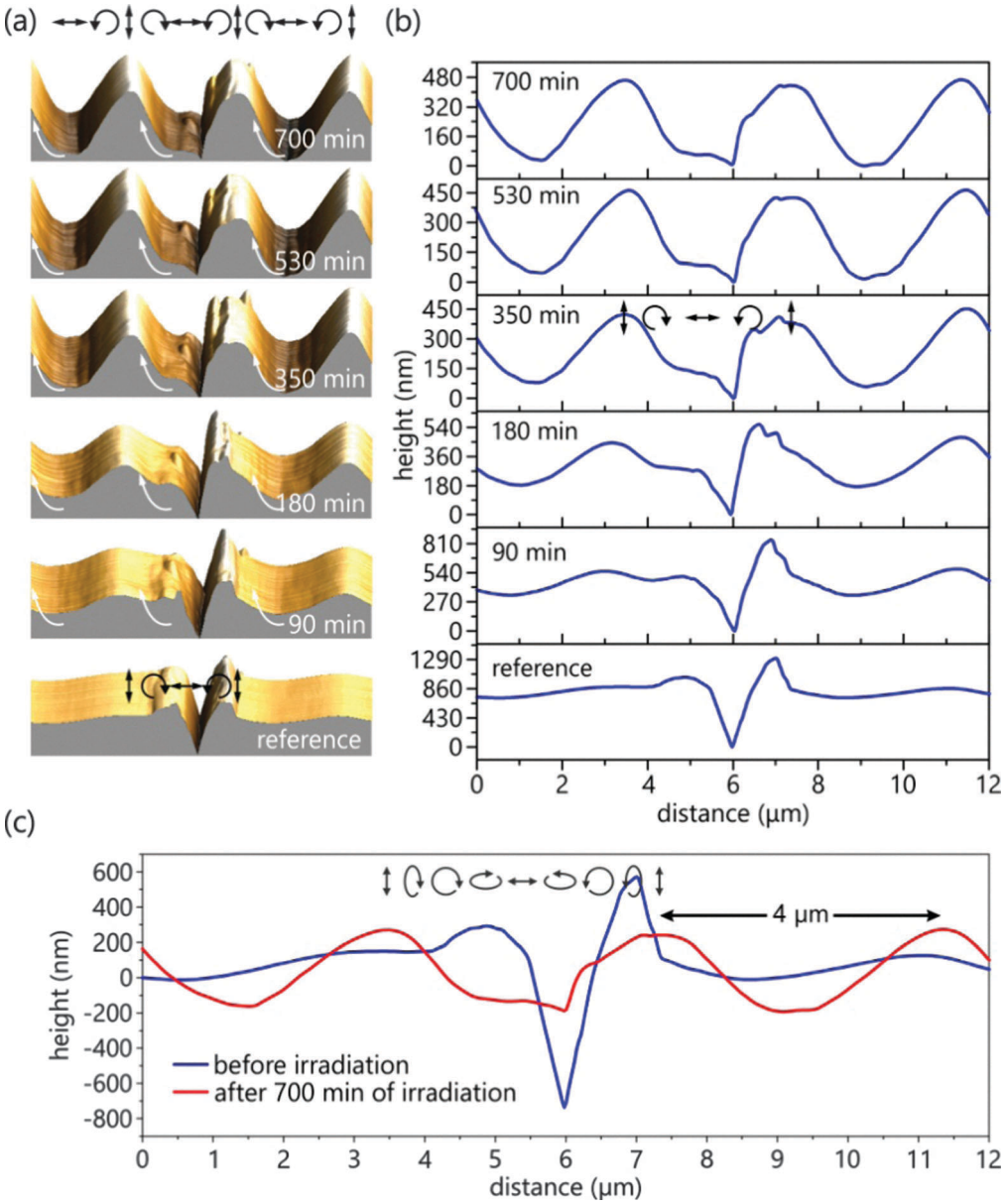

Fig. 8 *In situ* observation of SRG formation in the PAZO film using ±45° interference patterns. (a) AFM micrographs of the groove are shown as a function of irradiation time (bottom to top). (b) The corresponding cross-sectional profiles (bottom to top).

after irradiation stays constant. This behaviour is typical for elastic deformation of the bonded rubber-like rectangular piece.[48,49] This kind of deformation indicates visco-elastic/plastic behaviour rather than fluidization. Indeed, the simple concept of fluidization and flow is not appropriate to describe stretching in one direction and shrinking in orthogonal one; there should be a force that directs material displacement in one direction.

Similar stretching along the electrical field vector and compression in the perpendicular direction were reported for free floating azobenzene containing polymer films.[10,50] Lee *et al.* have reported a similar behaviour for the rectangular posts made of an epoxy based amorphous polymer, poly(disperse orange) 3 printed on a solid surface.[51] However, they interpreted this result as a light induced photo-fluidization process.

All the findings described above can be explained in the frame of the orientation approach at which the azobenzene chromophores reorient under irradiation perpendicularly to the electrical field vector causing the reorientation of the polymer backbone and as a consequence either elongation or contraction of the polymer material along the electrical field vector.[35,36,38,52–54] The sign of material deformation, *i.e.* contraction or elongation, depends on the chemical structure included in the theory as an angle between the azobenzene chromophores and the polymer main chain. If the azobenzene side chains are preferentially oriented perpendicularly to the main chain, the elongation along the electrical field vector takes place. In the case of smaller angles between photosensitive side chains and a polymer backbone, contraction of the polymer material along the electrical field vector

occurs. In our recent publication, we have indeed shown that in the case of amorphous polymer consisting of a PEI backbone and ionically bound azobenzene side chains, the polymer film shows out-of-phase behaviour, *i.e.* the grating maxima appear at the intensity maxima.[39] Similar behaviour was found also for polymer 2 (Azo-PCMS) (Fig. S3, ESI†) and polymer 3 (PAZO) (Fig. S4, ESI†).

To check whether the erasure of a scratch area can be induced at least partially by interference patterns, we have performed the experiment in which cross-scratched lines were irradiated with $\pm 45^{\circ}$ interference patterns. We aligned our set-up in such a way, that the vertically polarized electrical field vector ($\updownarrow$) is positioned exactly at the right edge of groove 1 (Fig. 7a and b). The results are shown for the PAZO polymer, the other two polymers Azo-Psi and Azo-PCMS obey similar behaviour. After irradiation for 1 hour one can see that the SRG developed with the grating vector pointing along groove 1 (Fig. 7b). In places of topography maxima groove 1 is locally closed at the positions where the E-field vector points perpendicularly to the groove. Similar results were published by Lee *et al.*, where the stripes of the azobenzene containing polymers were irradiated with UV interference patterns.[25] However, in our experiment when examining groove 2, one can see that it closes as well (observe SRG maxima) although the electrical field vector points ($\leftrightarrow$) along the groove. When considering a reaction of the polymer topography on the local variation of the electrical field vector along the grating direction, one can state that on the areas of the horizontal polarization (having the electric field vector ($\leftrightarrow$) parallel to the grating vector direction ($\leftrightarrow$)) the polymer film elongates along $\vec{E}$. This in turn results in "pushing" the polymer material towards places of vertical electrical field orientation and thus closing the groove 2.

We should mention, however that since the illumination is done using polarization interference patterns ($\pm 45^{\circ}$), at which the intensity stays constant along the grating vector, the global deformation of the polymer film is a complex interplay of the local reorientation of the azobenzene groups and the related reorientation of the polymer chains. Indeed, in the next experiment we aligned the interference pattern so that the horizontal polarization is positioned at the left edge of the groove (Fig. 8). In this case in the frame of the photo-fluidization concept, one would expect closure of the groove at least from one side due to elongation of the polymer material along the horizontal polarization. However, we have observed that the groove was opened by the contraction of the left edge of the groove (Fig. 8b and c). This again fails to support the photo-fluidization concept, and rather indicates the visco-elastic/plastic behaviour of the polymer film, at which anisotropic light-induced stress results in polymer film deformation.

4. Conclusions

We have investigated the response of three photosensitive polymer films to irradiation with interference patterns (IPs) and homogeneous light using our home-made set-up combining the optical part and an atomic force microscope (AFM). This set-up allows studying the evolution of the film deformation *in situ*, *i.e.* under continuous irradiation. It is also possible to assign the local topography change to the distribution of the electrical field vector within the interference pattern. The polymers were selected to have different glass transition temperatures (T_g). The studied polymers Azo-Psi, Azo-PCMS and PAZO have T_g of 32 °C, 87 °C and 95 °C, respectively.

The response of the polymers to irradiation with IP depends on the electric field vector distribution of the interference pattern. We have found that independent of the T_g the response to irradiation with intensity interference patterns (IIPs: SS, PP, RR, LL) is comparable in terms of the kinetic growth and the value of the grating height for all three polymers. In the case of illumination with polarization interference patterns (PIPs: $\pm 45^{\circ}$, RL), the maximal grating height measured at saturation of the SRG growth is higher for all three polymers than in the case of IIP irradiation. The polymer with higher glass transition temperature (Azo-PCMS) develops up to larger SRG, *i.e.* the maximal grating height is *ca.* 3 times higher than in the case of Azo-Psi. The stronger response is attributed to stronger coupling between the polymer main chain and active azobenzene side chains reorienting under irradiation, than in the case of Azo-Psi.

We also demonstrated the ability of the azobenzene containing polymeric films to switch the topography during changing irradiation conditions, which is a very interesting property for the biological field. This unique behaviour, characteristic only of the azobenzene containing materials,[55–58] will permit the generation of dynamically fluctuating surfaces[59–61] (modification of the surface relief geometric characteristics during the cell culture cycle). The use of reconfigurable dynamic surfaces will permit the separation of the influence of the mechanical signals transmitted by the surface to the cells and understand the transduction mechanisms (translation of the mechanical signals into chemical signals).[62]

In the second part of the manuscript, we have reported the study of the deformation of the rectangular piece of the polymer material cut/isolated out of the whole film under irradiation with light of certain polarization and homogeneous intensity distributions. For all three polymers we have found that the rectangular piece stretches along the electrical field vector and simultaneously shrinks in the perpendicular direction.

Our experiments support the re-orientation approach proposed by Saphiannikova *et al.*,[35,36] which is based on the idea that the reorientation of azobenzene molecules perpendicular to the light polarization causes the reorientation of polymer backbones, and thus the macroscopic deformation of a sample due to the strong mechanical coupling between the two phases: the passive polymer matrix and active azobenzenes.

References

1 P. Rochon, E. Batalla and A. Natansohn, *Appl. Phys. Lett.*, 1995, **66**, 136–138.
2 D. Y. Kim, S. K. Tripathy, L. Li and J. Kumar, *Appl. Phys. Lett.*, 1995, **66**, 1166–1168.
3 P. S. Ramanujam, N. C. R. Holme and S. Hvilsted, *Appl. Phys. Lett.*, 1996, **68**, 1329–1331.
4 N. C. R. Holme, L. Nikolova, S. Hvilsted, P. H. Rasmussen, R. H. Berg and P. S. Ramanujam, *Appl. Phys. Lett.*, 1999, **74**, 519–521.

5 J. E. Koskela, J. Vapaavuori, R. H. A. Ras and A. Priimagi, *ACS Macro Lett.*, 2014, **3**, 1196–1200.
6 A. Goulet-Hanssens, T. C. Corkery, A. Priimagi and C. J. Barrett, *J. Mater. Chem. C*, 2014, **2**, 7505–7512.
7 J. Vapaavuori, A. Goulet-Hanssens, I. T. S. Heikkinen, C. J. Barrett and A. Priimagi, *Chem. Mater.*, 2014, **26**, 5089–5096.
8 A. Emoto, E. Uchida and T. Fukuda, *Polymers*, 2012, **4**, 150.
9 C. J. Barrett, J.-i. Mamiya, K. G. Yager and T. Ikeda, *Soft Matter*, 2007, **3**, 1249–1261.
10 D. Bublitz, M. Helgert, B. Fleck, L. Wenke, S. Hvilsted and P. S. Ramanujam, *Appl. Phys. B: Lasers Opt.*, 2000, **70**, 863–865.
11 N. Akamatsu, W. Tashiro, K. Saito, J.-i. Mamiya, M. Kinoshita, T. Ikeda, J. Takeya, S. Fujikawa, A. Priimagi and A. Shishido, *Sci. Rep.*, 2014, **4**, 5377.
12 T. Papke, N. S. Yadavalli, C. Henkel and S. Santer, *ACS Appl. Mater. Interfaces*, 2014, **6**, 14174–14180.
13 T. König, T. Papke, A. Kopyshev and S. Santer, *J. Mater. Sci.*, 2013, **48**, 3863–3869.
14 T. Konig, Y. Nataraja Sekhar and S. Santer, *J. Mater. Chem.*, 2012, **22**, 5945–5950.
15 T. König, N. Yadavalli and S. Santer, *Plasmonics*, 2012, **7**, 535–542.
16 K. Tobias and S. Svetlana, *Nanotechnology*, 2012, **23**, 155301.
17 P. Karageorgiev, D. Neher, B. Schulz, B. Stiller, U. Pietsch, M. Giersig and L. Brehmer, *Nat. Mater.*, 2005, **4**, 699–703.
18 N. Hurduc, B. C. Donose, A. Macovei, C. Paius, C. Ibanescu, D. Scutaru, M. Hamel, N. Branza-Nichita and L. Rocha, *Soft Matter*, 2014, **10**, 4640–4647.
19 N. Mechau, M. Saphiannikova and D. Neher, *Appl. Phys. Lett.*, 2006, **89**, 251902.
20 M. Grenzer, *Habilitation thesis*, University of Potsdam, 2007.
21 J. M. Harrison, D. Goldbaum, T. C. Corkery, C. J. Barrett and R. R. Chromik, *J. Mater. Chem. C*, 2015, **3**, 995–1003.
22 J. Brandrup, E. H. Immergut and E. A. Grulke, *Polymer Handbook*, Wiley-Interscience, 1 edn, 2003.
23 A. Shimamura, A. Priimagi, J. Mamiya, T. Ikeda, Y. Yu, C. J. Barrett and A. Shishido, *ACS Appl. Mater. Interfaces*, 2011, **3**, 4190–4196.
24 M. Saphiannikova and V. Toshchevikov, *J. Soc. Inf. Disp.*, 2015, **23**, 146–153.
25 S. Lee, H. S. Kang and J.-K. Park, *Adv. Mater.*, 2012, **24**, 2069–2103.
26 G. Di Florio, E. Brundermann, N. S. Yadavalli, S. Santer and M. Havenith, *Soft Matter*, 2014, **10**, 1544–1554.
27 F. Lagugne-Labarthet, *Annu. Rep. Prog. Chem., Sect. C: Phys. Chem.*, 2007, **103**, 326–350.
28 F. L. Labarthet, T. Buffeteau and C. Sourisseau, *J. Appl. Phys.*, 2001, **90**, 3149–3158.
29 G. D. Florio, E. Bründermann, N. S. Yadavalli, S. Santer and M. Havenith, *Nano Lett.*, 2014, **14**, 5754–5760.
30 T. A. Singleton, K. S. Ramsay, M. M. Barsan, I. S. Butler and C. J. Barrett, *J. Phys. Chem. B*, 2012, **116**, 9860–9865.
31 A. Kopyshev, C. J. Galvin, J. Genzer, N. Lomadze and S. Santer, *Langmuir*, 2013, **29**, 13967–13974.
32 C. Schuh, N. Lomadze, J. Rühe, A. Kopyshev and S. Santer, *J. Phys. Chem. B*, 2011, **115**, 10431–10438.
33 N. Lomadze, A. Kopyshev, J. Rühe and S. Santer, *Macromolecules*, 2011, **44**, 7372–7377.
34 A. Kopyshev, N. Lomadze, D. Feldmann, J. Genzer and S. Santer, *Polymer*, 2015, **79**, 65–72.
35 V. Toshchevikov and M. Saphiannikova, *J. Phys. Chem. B*, 2014, **118**, 12297–12309.
36 V. Toshchevikov, M. Saphiannikova and G. Heinrich, *J. Phys. Chem. B*, 2012, **116**, 913–924.
37 J. M. Ilnytskyi, D. Neher and M. Saphiannikova, *J. Chem. Phys.*, 2011, **135**, 044901.
38 V. Toshchevikov, M. Saphiannikova and G. Heinrich, *J. Phys. Chem. B*, 2009, **113**, 5032–5045.
39 N. S. Yadavalli, T. Konig and S. Santer, *J. Soc. Inf. Disp.*, 2015, **23**, 154–162.
40 N. S. Yadavalli, M. Saphiannikova and S. Santer, *Appl. Phys. Lett.*, 2014, **105**, 051601.
41 N. S. Yadavalli, D. Korolkov, J.-F. Moulin, M. Krutyeva and S. Santer, *ACS Appl. Mater. Interfaces*, 2014, **6**, 11333–11340.
42 N. S. Yadavalli and S. Santer, *J. Appl. Phys.*, 2013, **113**, 224304.
43 N. Yadavalli, M. Saphiannikova, N. Lomadze, L. Goldenberg and S. Santer, *Appl. Phys. A: Mater. Sci. Process.*, 2013, **113**, 263–272.
44 K. Kazmierski, N. Hurduc, G. Sauvet and J. Chojnowski, *J. Polym. Sci., Part A: Polym. Chem.*, 2004, **42**, 1682–1692.
45 Q. Ferreira, P. A. Ribeiro, O. N. Oliveira and M. Raposo, *ACS Appl. Mater. Interfaces*, 2012, **4**, 1470–1477.
46 F. Lagugné-Labarthet, C. Sourisseau, R. D. Schaller, R. J. Saykally and P. Rochon, *J. Phys. Chem. B*, 2004, **108**, 17059–17068.
47 F. L. Labarthet, J. L. Bruneel, T. Buffeteau and C. Sourisseau, *J. Phys. Chem. B*, 2004, **108**, 6949–6960.
48 A. N. Gent and E. A. Meinecke, *Polym. Eng. Sci.*, 1970, **10**, 48–53.
49 A. N. Gent and P. B. Lindley, *Proc. - Inst. Mech. Eng.*, 1959, **173**, 111–117.
50 M. Helgert, B. Fleck, L. Wenke, S. Hvilsted and P. S. Ramanujam, *Appl. Phys. B: Lasers Opt.*, 2000, **70**, 803–807.
51 H. S. Kang, H.-T. Kim, J.-K. Park and S. Lee, *Adv. Funct. Mater.*, 2014, **24**, 7273–7283.
52 V. P. Toshchevikov, M. Saphiannikova and G. Heinrich, *J. Chem. Phys.*, 2012, **137**, 024903.
53 V. P. Toshchevikov, M. Saphiannikova and G. Heinrich, *Proc. SPIE*, 2012, **8545**, 854507.
54 M. Saphiannikova, V. Toshchevikov and J. Ilnytskyi, *Nonlinear Opt., Quantum Opt.*, 2010, **41**, 27–57.
55 C. Rianna, M. Ventre, S. Cavalli, M. Radmacher and P. A. Netti, *ACS Appl. Mater. Interfaces*, 2015, **7**, 21503–21510.
56 C. Rianna, A. Calabuig, M. Ventre, S. Cavalli, V. Pagliarulo, S. Grilli, P. Ferraro and P. A. Netti, *ACS Appl. Mater. Interfaces*, 2015, **7**, 16984–16991.
57 J. Vapaavuori, R. H. A. Ras, M. Kaivola, C. G. Bazuin and A. Priimagi, *J. Mater. Chem. C*, 2015, **3**, 11011–11016.
58 J. J. Gooding, S. G. Parker, Y. Lu and K. Gaus, *Langmuir*, 2014, **30**, 3290–3302.
59 S. A. Prokhorova, A. Kopyshev, A. Ramakrishnan, H. Zhang and J. Rühe, *Nanotechnology*, 2003, **14**, 1098.
60 S. Santer and J. Rühe, *Polymer*, 2004, **45**, 8279–8297.
61 S. Santer, A. Kopyshev, J. Donges, H. K. Yang and J. Rühe, *Adv. Mater.*, 2006, **18**, 2359–2362.
62 P. M. Tsimbouri, *J. Funct. Biomater.*, 2015, **6**, 598–622.